

Magnetoelastic effects in multiferroic HoMnO₃

Tapan Chatterji¹, Thomas Hansen¹, Simon A.J. Kimber² and Dipten Bhattacharya³

¹*Institut Laue-Langevin, B.P. 156, 38042 Grenoble Cedex 9, France*

²*European Synchrotron Radiation Facility, B.P. 220, 38043 Grenoble Cedex 9, France*

³*Central Glass and Ceramic Research Institute, Kolkata 700032, India*

(Dated: November 2, 2018)

We have investigated magnetoelastic effects in multiferroic HoMnO₃ below the antiferromagnetic phase transition $T_N \approx 75$ K by neutron powder diffraction. The lattice parameter a of the hexagonal unit cell of HoMnO₃ decrease in the usual way at lower temperatures and then shows abrupt contraction below T_N whereas the lattice parameter c increases continuously with decreasing temperature and shows an anomalous increase below T_N . The unit cell volume decreases continuously with decreasing temperature and undergoes abrupt contraction below T_N . By fitting the background thermal expansion for a nonmagnetic lattice with the Einstein-Grüneisen equation we determined the lattice strains Δa , Δc and ΔV due to the magnetoelastic effects as a function of temperature. We have also determined the temperature variation of the ordered magnetic moment of Mn ion by fitting the measured Bragg intensities of the nuclear and magnetic reflections with the known crystal and magnetic structure models.

PACS numbers: 61.05.fm, 65.40.De

One of the most challenging subjects of the condensed matter physics is the coupling between spin and lattice degrees of freedom. The spin system in ferromagnetic or antiferromagnetic crystals is coupled to the ionic displacements via the dependence on distance of the exchange interaction or spin-orbit or dipole-dipole interaction. The coupling is called the magnetoelastic coupling and resultant effects are called magnetoelastic effects¹⁻³. The static part of this effect is the shift in the equilibrium ionic positions with resultant displacements of the phonon and magnon spectra. The dynamic part of this interaction is the magnon-phonon scattering and also their hybridization. The simplest static part of the interaction is the external magnetostriction, or the change in macroscopic crystal dimensions. This changes the lattice parameters below the magnetic phase transition and can be more easily determined experimentally. In addition there are shifts in the atomic coordinates within each unit cell. This is called internal magnetostriction which is more difficult to measure. The induced atomic displacements may or may not modify the symmetry of the lattice and also the anisotropic energy. There exist a large number of review articles that summarize the experimental results and also to some extent some theoretical calculations⁴⁻⁸. The magnetoelastic effect has drawn renewed interest in connection with the potentially useful colossal magnetoresistive and multiferroic materials. Here we have investigated the magnetostriction in multiferroic hexagonal manganite HoMnO₃.

HoMnO₃ belongs to the family of hexagonal manganites RMnO₃ (R = Sc, Y, Er, Ho, Tm, Yb, Lu) that show multiferroic behaviour⁹. These hexagonal manganites are paraelectric at high temperatures with the centrosymmetric space group $P6_3/mmc$. Below about 1000 K they undergo a paraelectric-to-ferrielectric transition to a non-centrosymmetric structure with the space group $P6_3cm$. At further lower temperatures of the or-

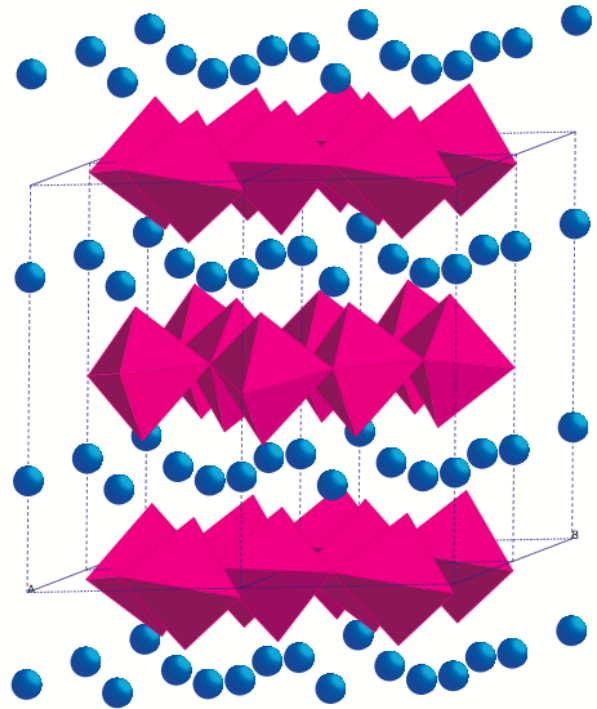


FIG. 1: (Color online) Schematic representation of the hexagonal crystal structure of RMnO₃ (R = Sc, Y, Er, Ho, Tm, Yb, Lu). Here we have used the structural parameters for HoMnO₃. The red trigonal bipyramids represent Mn ions surrounded by five O atoms and the blue spheres are Ho ions.

der of about 100 K the magnetic hexagonal manganites order with a non-collinear antiferromagnetic structure with propagation vector $\mathbf{k} = 0$. Among these hexagonal manganites YMnO₃ and HoMnO₃ have been investigated quite intensively¹⁰⁻¹⁶. We have performed neutron powder diffraction investigation of the temperature depen-

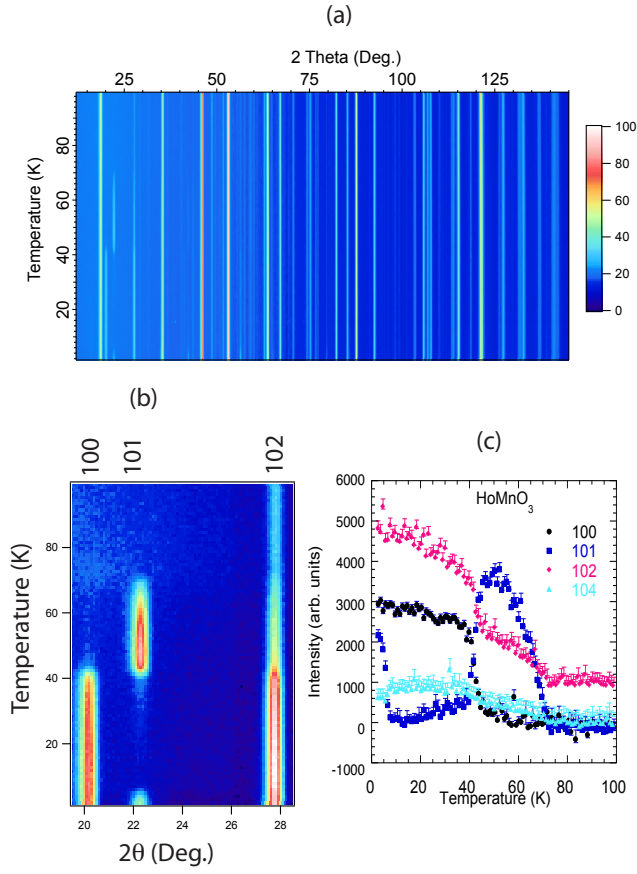


FIG. 2: (Color online) (a) Temperature variation of the diffraction intensities of HoMnO_3 . (b) Temperature variation of a few low angle reflections from HoMnO_3 containing magnetic contributions. (c) Temperature variation of the peak intensity of the 100, 101, 102 and 104 reflections.

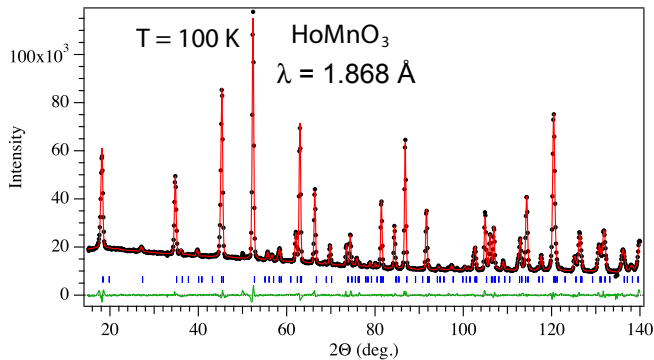


FIG. 3: (Color online) Results of the refinement of the hexagonal crystal structure of HoMnO_3 at $T = 100$ K. The tick marks below the diffraction pattern show the calculated positions of the diffraction peaks and the difference between the observed and calculated intensities has been plotted below the tick marks.

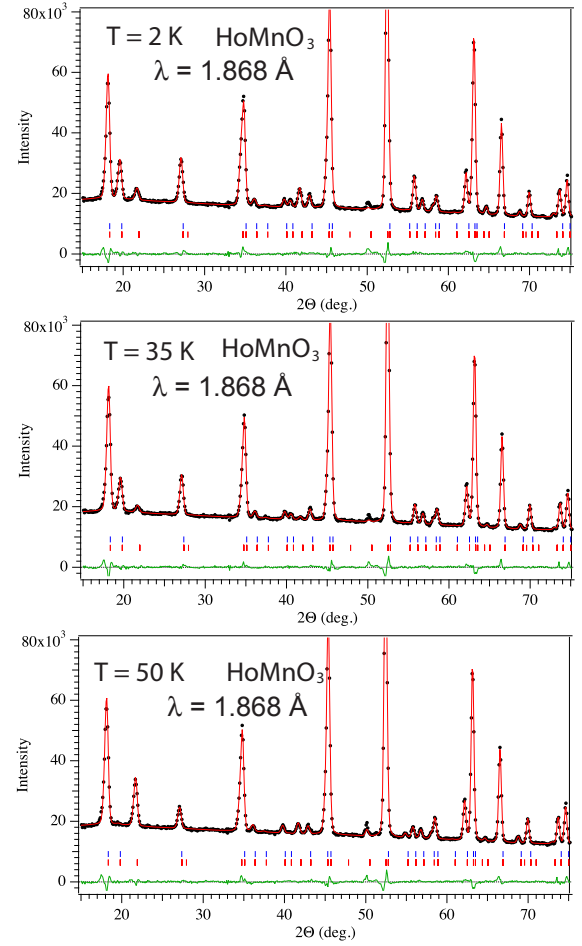


FIG. 4: (Color online) Results of the refinement of the crystal and magnetic structures of HoMnO_3 at $T = 2, 35$ and 50 K. The upper tick marks below the diffraction pattern show the calculated positions of the nuclear peaks and the lower tick marks show the calculated positions of the magnetic peaks. The difference between the observed and calculated intensities has been plotted below the tick marks.

dence of the crystal and magnetic structure of HoMnO_3 . Here we report the observation of considerable magnetoelastic effects below the Néel temperature $T_N \approx 75$ K.

In order to determine quantitatively the magnetoelastic effect or the spontaneous magnetostriction one needs to measure very accurately the temperature variation of the lattice parameters and the unit cell volume in small temperature steps. These temperature variations often reveal anomalous behavior around the magnetic ordering temperature. To extract the magnetoelastic effect one needs to know the background temperature variation in the absence of magnetoelastic effect in a fictitious non-magnetic solid which otherwise resembles the compound under study. This is not an easy task and the disagreements between experimental results often arise from the procedure of determination of the background temperature variation of the lattice parameters. One

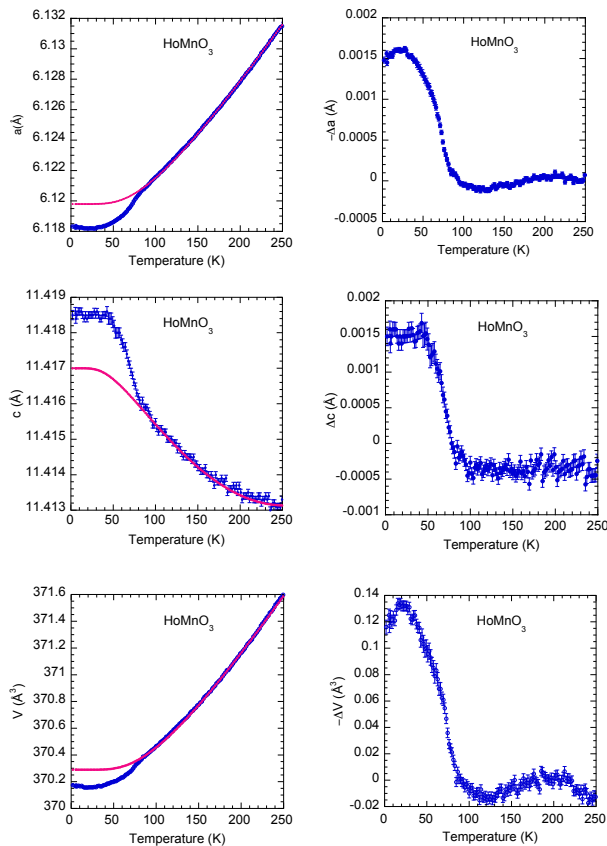


FIG. 5: (Color online) Temperature variation of the lattice parameters a , c , and the unit cell volume V of HoMnO_3 plotted on the left panel. The red curves in these figures represent the lattice parameter and the unit cell volume obtained by fitting the high temperature data by a Einstein-Grüneisen equation and extrapolated to the low temperature. This should give the background for the non-magnetic lattice. On the right panel the temperature dependence of the lattice strains Δa and ΔV obtained by subtracting the non-magnetic background have been plotted.

of the commonly employed method is to fit the high temperature data above the ordering temperature by the Debye equation in the Grüneisen approximation¹⁷ or the simpler Einstein equation in the same Grüneisen approximation¹⁸ and then extrapolating to the lower temperatures to give the background variations in the absence of magnetism. The simpler Einstein-Grüneisen equation¹⁸ serves as an excellent fit function for not only the volume but also for the individual lattice parameters and we have used it here.

Neutron diffraction experiments were done on HoMnO_3 on the high intensity powder diffractometer D20¹⁹ of the Institute Laue-Langevin in Grenoble. The 115 reflection from a Ge monochromator at a high take-off angle of 118° gave a neutron wavelength of 1.868 \AA .

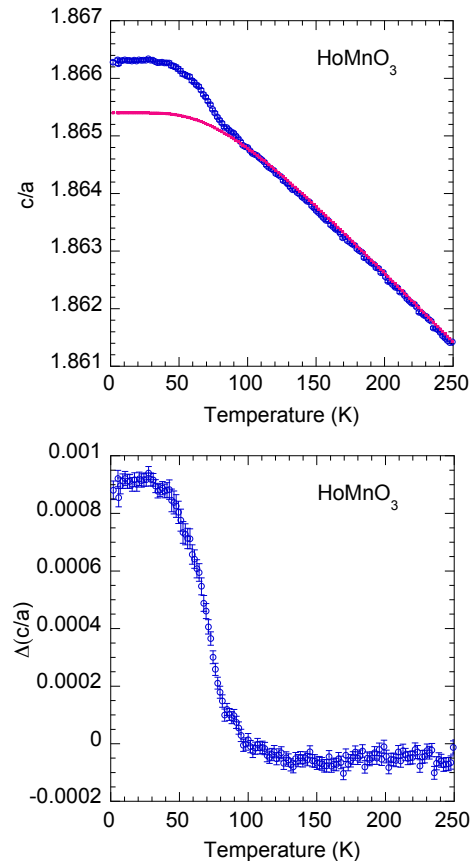


FIG. 6: (Color online) Temperature variation of the $\frac{c}{a}$ ratio of HoMnO_3 plotted on the upper panel. The red curves in these figures represent the $\frac{c}{a}$ ratio obtained by fitting the high temperature data by the Einstein-Grüneisen function and extrapolated to the low temperature. It is assumed that this gives the temperature variation of $\frac{c}{a}$ for the non-magnetic lattice. On the bottom panel the temperature dependence of the $\frac{c}{a}$ ratio obtained by subtracting the non-magnetic background have been plotted.

Approximately 5 g of HoMnO_3 powder sample was placed inside an 8 mm diameter vanadium can, which was fixed to the sample stick of a standard ^4He cryostat. We have measured the diffraction intensities from HoMnO_3 as a function of temperature in the range 2 – 300 K. Fig. 2 (a) shows the temperature variation of the diffraction intensities of HoMnO_3 . The temperature variation of a few low angle reflections from HoMnO_3 containing magnetic contributions is shown in Fig. 2 (b) and the temperature variation of the peak intensities of the 100, 101, 102 and 104 reflections is shown in Fig. 2 (c). The temperature variation of the intensities of the low angle reflections from HoMnO_3 clearly shows two magnetic phase transitions, one at the Néel temperature $T_N \approx 75 \text{ K}$ and the second spin reorientation transition at about $T_{SR} \approx 40 \text{ K}$.

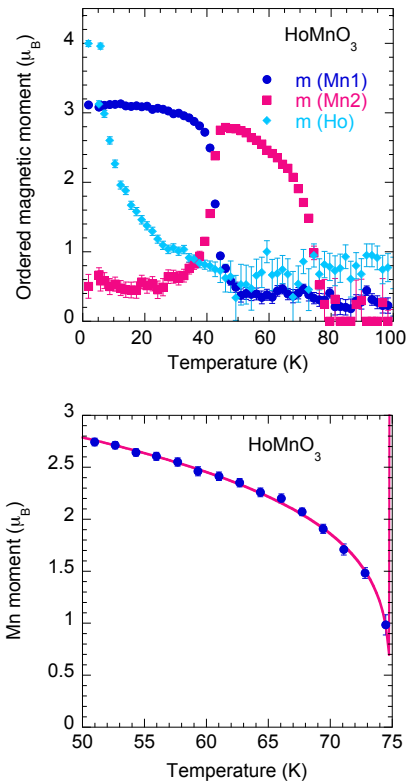


FIG. 7: (Color online) (Upper panel) Temperature variation of the ordered magnetic moment m (Mn1) and m (Mn2) of Mn and m (Ho) of Ho ions of HoMnO_3 obtained by fitting the measured Bragg intensities of the nuclear and magnetic reflections with the known crystal and magnetic structure models. m (Mn1) is the ordered magnetic moment corresponding to the spin rotated low temperature phase below $T_{SR} \approx 40$ K and m (Mn2) is the ordered magnetic moment of the higher temperature magnetic phase that develops below $T_N \approx 75$ K and undergoes a phase transition below $T_{SR} \approx 40$ K to the spin reoriented low temperature phase. (Lower panel) Power-law fit of the temperature variation of m (Mn2) data close to T_N .

Rietveld refinement²⁰ of crystal and magnetic structures against the experimental diffraction data was done by the Fullprof program²¹. The refinement results from HoMnO_3 at $T = 100$ K in the paramagnetic state are shown in Fig. 3. At $T = 100$ K only the nuclear Bragg peaks were observed and the refinement of the nuclear structure was done by the known crystal structure of the hexagonal manganites^{12,13}. Fig. 4 shows the results of refinement of the crystal and magnetic structures^{13,14} at $T = 2, 35$ and 50 K in the three magnetic phases of HoMnO_3 . The agreement factors and χ^2 values of these refinements are given in Table I. It is to be noted that magnetic structures of hexagonal manganites including HoMnO_3 show homometry, which cannot be distinguished by powder neutron diffraction. Only po-

larized neutron diffraction on single crystals can resolve the homometric structures¹⁴.

TABLE I: Agreement factors for the refinement of crystal and magnetic structures of HoMnO_3 at different temperatures. R_p and R_{wp} are the unweighted and weighted agreement or R factors whereas the R_{exp} is the expected R factor corresponding to the statistics of the data and χ^2 has the usual statistical meaning.

$T(K)$	$R_p(\%)$	$R_{wp}(\%)$	$R_{exp}(\%)$	χ^2
2	8.13	7.11	3.15	5.10
35	8.04	7.03	3.20	4.82
50	8.53	7.38	3.22	5.26
100	8.84	7.35	3.30	4.98

Figure 5 shows the temperature variation of the lattice parameters a , c , and the unit cell volume V of HoMnO_3 plotted on the left panel. The lattice parameter a decreases continuously with decreasing temperature in a very normal way, but close to the Néel temperature $T_N \approx 75$ K shows the magnetoelastic or magnetostriction anomaly. The red curve represent the background variation of the a lattice parameter for a nonmagnetic solid obtained by fitting the data in the paramagnetic state by the Einstein-Grüneisen equation explained before. By subtracting the background from the data we determined the lattice strain Δa plotted on the right panel of Figure 5. The c lattice parameter increases continuously on decreasing temperature down to T_N and then shows abrupt anomalous increase or positive magnetostriction. By subtracting the background variation of the c lattice parameter (red continuous curve) from the data we determined the lattice strain Δc plotted on the right panel. Similar plots for the unit cell volume V and the volume strain ΔV are shown in Figure 5 in the left and the right panels, respectively. Fig. 6 shows in the upper panel the temperature dependence of the $\frac{c}{a}$ ratio. It varies linearly with temperature above about 100 K and below this temperature the $\frac{c}{a}$ shows anomalous behavior due the magnetoelastic effect. However we fitted the $\frac{c}{a}$ ratio above 100 K by the Einstein-Grüneisen equation and extrapolated to the lower temperature. The fit is shown by the red line. Fig 6 shows in the lower panel the difference between the observed and the fitted $\frac{c}{a}$ ratio. It is evident that the temperature variation of $\frac{c}{a}$ also behave like the other lattice parameters with respect to the magnetoelastic effect. We note that although the magnetic ordering temperature of HoMnO_3 is $T_N \approx 75$ K, the magnetoelastic effect starts becoming appreciable already below about $T^* \approx 100$ K. This appearance of magnetoelastic effect already about 25 K above $T_N \approx 75$ K is due to short-range spin correlations. The spontaneous linear magnetostriction along the a-axis at $T = 0$ is $\Delta a/a_0 = -2.45 \times 10^{-4}$ and that along the c-axis is $\Delta c/c_0 = 1.31 \times 10^{-4}$. The spontaneous volume magnetostriction in HoMnO_3 is $\Delta V/V_0 = -3.51 \times 10^{-4}$.

We can calculate the spontaneous volume magnetorestriction in HoMnO₃ from $\Delta V/V_0 = 2\Delta a/a_0 + \Delta c/c_0 = -3.59 \times 10^{-4}$ which very close to that obtained from the unit cell volume variation $\Delta V/V_0 = -3.51 \times 10^{-4}$. This suggests that our method of extracting magnetoelastic effect is reliable or at least consistent. The magnitude of spontaneous magnetostriction in HoMnO₃ is relatively large and is comparable to those²² determined in the other multiferroic hexagonal manganite YMnO₃.

Figure 7 (a) shows the temperature variation of the ordered magnetic moments m of Mn ion corresponding to the high temperature magnetic phase of HoMnO₃ (shown by the red filled squares) and lower temperature spin reoriented phase of HoMnO₃ (shown by filled blue circles) obtained by fitting the measured Bragg intensities of the nuclear and magnetic reflections with the known crystal and magnetic structure models. The ordered magnetic moment of the high temperature magnetic phase decreases with increasing temperature above about the spin reorientation transition temperature $T_{SR} \approx 40$ K in the usual way and becomes zero at $T_N \approx 75$ K. Below $T_{SR} \approx 40$ K the moment of this phase decreases and the magnetic moment of the spin reoriented low temperature phase increases abruptly and becomes saturated to about $3.1\mu_B$ at $T = 2$ K. The Ho magnetic moment is polarized at all temperatures below $T_N \approx 75$ K but below about 50 K the Ho moment increases with decreasing temperature and becomes about $4\mu_B$ at $T = 2$ K. The temperature variation of the ordered magnetic moment of the Ho sublattice resembles the Brillouin function and indicates strongly the absence of any magnetic phase transition¹⁵ in HoMnO₃ at lower temperatures. Figure 7 (b) shows the power-law fit of the magnetic moment of Mn in the higher temperature phase of HoMnO₃ below $T_N \approx 75$ K. We have included the data points in the temperature range 50-74 K. The least squares fit of these data gave the power-law exponent $\beta = 0.247 \pm 0.005$ and

$T_N = 74.84 \pm 0.05$ K. Since there are no data close to T_N the the power-law exponent obtained cannot be associated really with the critical exponent. However the determined Néel temperature $T_N = 74.84 \pm 0.05$ K from the fit is dependable within the experimental resolution. It is to be noted that the magnetoelastic effects shown in Fig. 5 in the lattice parameters are not sensitive to the spin-reorientation transition at $T_{SR} \approx 40$ K. It is not quite sure whether the ordered magnetic moment of the Ho sublattice at lower temperature influence the magnetoelastic effect substantially.

The temperature variations of the lattice strains determined in HoMnO₃ do not look very smooth and do not become zero above $T_N \approx 75$ K. This is partly due to the problem of determining the background temperature variation of the lattice parameters and unit cell volume by the Einstein-Grüneisen function and also may be due to multiple magnetic phase transitions and the polarization of the Ho magnetic moments. We could not therefore relate quantitatively the lattice strain and the magnetic order parameter as we did in YMnO₃ and other simple antiferromagnetic systems²²⁻²⁴. We checked carefully whether we could get any information about the shifts in atomic coordinates in the unit cell below the magnetic ordering temperature or the internal magnetoelastic effect. Although the agreement factors of the refinement of the crystal and magnetic structures against the data were reasonably good (see Table I), the resulting positional parameters do not show within the refinement accuracy any anomalous shifts in atomic coordinates below T_N .

In conclusion we have measured accurately neutron diffraction intensities of HoMnO₃ powder sample and determined the magnetostriction below the magnetic ordering temperature. We have also determined the magnetic phase transitions and the temperature evolution of the magnetic moments of Mn and Ho ions.

-
- ¹ R. Becker and W. Döring, *Ferromagnetismus* (Verlag Julius Springer, Berlin, 1939)
 - ² E.R. Callen and H.B. Callen, Phys. Rev. B **129**, 578 (1963).
 - ³ E.R. Callen and H.B. Callen, Phys. Rev. B **139**, A455 (1963).
 - ⁴ E.W. Lee, Rep. Prog. Phys. **18**, 184 (1955).
 - ⁵ A.E. Clark, *Ferromagnetic Materials*, ed. E.P. Wohlfarth, North-Holland Publishing Company (1980).
 - ⁶ A.V. Andreev, *Handbook of Magnetic Materials*, ed. K.H. Buschow, Elsevier, vol. 1, p. 531 (1995).
 - ⁷ A. Lindbaum and M. Rotter, *Handbook of Magnetic Materials*, ed. K.H. Buschow, Elsevier, vol. 14, p. 307 (2002).
 - ⁸ M. Doerr, M. Rotter and A. Lindbaum, Advances in Physics, **54**, 1 (2005).
 - ⁹ Z.J. Huang, Y. Cao, Y.Y. Sun, Y.Y. Xue and C.W. Chu, Phys. Rev. B **56**, 2623 (1997).
 - ¹⁰ E.F. Bertaut and M. Mercier, Phys. Lett. **5**, 27 (1963).
 - ¹¹ E. Bertat, R.Pauthenet, and M. Mercier, Phys. Lett. **18**, 13 (1967).
 - ¹² A. Munõz, J.A. Alonso, M.J. Martínez-Lope, M.T. Casáis, J.L. Martínez, and M.T. Fernández-Díaz, Phys. Rev. B **62**, 9498 (2000).
 - ¹³ A. Munõz, J.A. Alonso, M.J. Martínez-Lope, M.T. Casáis, J.L. Martínez, and M.T. Fernández-Díaz, Chem. Mater. **13**, 1497 (2001).
 - ¹⁴ P.J. Brown and T. Chatterji, J. Phys: Condens. Matter **18**, 10085 (2006).
 - ¹⁵ P.J. Brown and T. Chatterji, Phys. Rev. B **77**, 104407 (2008).
 - ¹⁶ B. B. van Aken, T.T.M. Palstra, A. Filippetti and N.A. Spaldin, Nature Materials **3**, 164 (2004).
 - ¹⁷ W.C. Wallace, *Thermodynamics of Crystals*, John Wiley & Sons, New York (1972).
 - ¹⁸ T. Chatterji and T.C. Hansen, J. Phys.: Condens. Matter **23**, 276007 (2011).
 - ¹⁹ T.C. Hansen, P.F. Henry, H.E. Fischer, J. Torregrossa and P. Convert, Meas. Sci. Technol. **19**, 034001 (2008).

- ²⁰ H.M. Rietveld, *J. Appl. Cryst.* **2**, 65 (1969).
- ²¹ J. Rodriguez-Carvajal, FULLPROF, a Rietveld and pattern matching and analysis program version 2010, LLB, CEA-CNRS, France [<http://www.ill.eu/sites/fullprof/>]
- ²² T. Chatterji, B. Ouladdiaf, P.F. Henry and D. Bhat-tacharya, *J. Phys.: Condensed Matter* **24**, 336003 (2012).
- ²³ T. Chatterji, G.N. Iles, B. Ouladdiaf and T.C. Hansen, *J. Phys.: Condensed Matter* **22**, 316001 (2010).
- ²⁴ T. Chatterji, B. Ouladdiaf and T.C. Hansen, *J. Phys.: Condensed Matter* **22**, 096001 (2010).